

Structure and static properties of indium nitride at low and moderate pressures

This article has been downloaded from IOPscience. Please scroll down to see the full text article.

1993 J. Phys.: Condens. Matter 5 6015

(<http://iopscience.iop.org/0953-8984/5/33/010>)

View [the table of contents for this issue](#), or go to the [journal homepage](#) for more

Download details:

IP Address: 171.66.16.159

The article was downloaded on 12/05/2010 at 14:20

Please note that [terms and conditions apply](#).

Structure and static properties of indium nitride at low and moderate pressures

A Muñoz† and K Kunc‡

† Departamento de Física Fundamental y Experimental, Universidad de La Laguna, 38204 La Laguna, Tenerife, Spain

‡ Laboratoire de Physique des Solides associé au CNRS, Université P et M Curie, Tour 13, Boîte 79, 4 Place Jussieu, 75252 Paris Cédex 05, France

Received 19 April 1993

Abstract. The $E(V)$ phase diagram of different crystal structures of indium nitride is studied theoretically, using density functional theory, pseudopotential and full-potential LMTO methods. The high-pressure phase is identified as rocksalt and is found to be semiconducting. The transition pressure is predicted, and the lattice constants, the internal distortion parameter of the wurtzite structure, the bulk modulus, the pressure derivative of the bulk modulus, and the equilibrium energies are obtained for both low- and high-pressure phases. Trends in the transition pressures are discussed.

1. Introduction

Structural properties of the group-III nitrides (BN, AlN, GaN) have been intensively studied, both experimentally [1–4] and theoretically [5–13]. Recently, interest has concentrated on the phase transition under high pressures. All works cited above agree on the existence of a phase transition in AlN and GaN, and all the theoretical calculations identify the structure of the high-pressure phase concordantly as the rocksalt modification. A conspicuous feature of the nitride series, nevertheless, is the absence of any clear trend in the transition pressure p_t : $\gg 1100$ GPa for BN [6, 7], 16–17 GPa in AlN [9, 10] and 55–65 GPa for GaN [11–13]. The nitrides are beyond the range within which the Chelikowsky theory [14] of phase transitions applies. We can nevertheless retain from [14], for *qualitative* reasoning, that the transition pressure tends to decrease (at constant ionicity) with the increasing bond length†. It is this tendency of p_t to decrease when progressing down a column in the periodic table that seems to be infringed by the nitrides, and one wonders whether it is the AlN transition pressure that is exceptionally low or the GaN pressure that is exceptionally high. As no answer can be given for a series consisting of only three elements, the fourth nitride is naturally brought into focus: InN.

Although very little is known about the physical properties of indium nitride at *any* pressure, the first attempts at experimentally establishing the phase transition were undertaken recently [15]. Until the quality of the samples improves so as to allow clear-cut conclusions with acceptable error margins, we propose to address the question using

† An attempt at discerning, from [14], a similar trend in the variation of p_t with ionicity f_i is less fruitful and does not bring a useful criterion for our systems. Keeping the bond length constant, p_t is expected to increase with f_i at low ionicities and to decrease at high ones. The difficulty with the nitrides is that the f_i of AlN and GaN (0.45 and 0.50 respectively) are close to the borderline where neither of the two rules applies.

theoretical tools, namely by means of *ab initio* calculations of total energy: we will evaluate the $E(V)$ equation of state for different structures of InN, establish the complete phase diagram and *predict* the transition pressure. Actually, InN has so far been so little studied that, even at ambient pressure, most of the physical characteristics are uncertain or unknown. We thus propose to supply some basic knowledge about InN in the wurtzite structure, which is the equilibrium low-pressure modification, even *before* experiment is able to do so: the 'internal' crystallographic parameters, the bulk modulus, and the electronic charge density distribution. These data will also be determined for the high-pressure structure.

2. Self-consistent calculations of energy

The total-energy calculations behind this work are based on density functional theory in the local density approximation [16] applied, on the one hand, in the plane-wave basis, and on the other hand in terms of muffin-tin orbitals (FP-LMTO). Applying the theory in the plane-wave basis, we use the norm-conserving pseudopotentials [17] and the Ceperley–Alder exchange–correlation [18]. The spin–orbit interactions are neglected and the eventual relativistic effects are accounted for approximately, owing to the procedures used in the design of the pseudopotentials [17]. Unless otherwise stated, the self-consistent calculations are performed with the plane-wave cutoff $E^{\text{PW}} = 70 \text{ Ryd}$ (4000 plane waves at the equilibrium volume of the wurtzite); for a few quantities we limited ourselves to 40 Ryd—the cutoff we used in the preliminary calculations. The high values of the cutoff energies are a consequence of the small size of the nitrogen orbitals and of the deep potential of the nitrogen core; they are consistent with the cutoffs we used in our previous work on GaN [11], and somewhat higher than those used by other authors on other III–V nitrides [9, 13, 19].

As the rigidity of the In core may be suspect, a possible polarization of the $4d^{10}$ orbitals comes to mind in analogy with that of the $3d^{10}$ electrons in Ga, we verified the main results by an all-electron method: the FP-LMTO (full-potential linear muffin-tin orbital) method [20]. In contrast to the well known LMTO-ASA [21], the FP-LMTO does not introduce any shape approximations for the potential or the charge density, and it does not assume a constant potential between the spheres; we apply this method under conditions similar to those, for example, in [22]; in particular, the orbitals $4d^{10}$, $5s^2$, $5p^1$ of In and $2s^2$, $2p^3$ of N are all included in the self-consistent treatment, i.e. viewed as valence electrons. Two or three basis functions per site and angular momentum are retained in the expansions ($3 \times s$, $3 \times p$, $2 \times d$, both for In and N). The muffin-tin radii are chosen equal at both cation and anion sites, and empty spheres are introduced. The Hedin–Lundqvist exchange correlation [23] is assumed and the relativistic effects are taken into account explicitly (a scalar-relativistic treatment [20]).

3. Static properties and phase diagram

We start by calculating the $E(V)$ for InN in a zincblende structure, assuming that the equation of state cannot be very different from that of wurtzite. Having calculated the total energy by the pseudopotential method at seven different lattice constants between 4.5 and 5.1 Å, we fit the results to the Murnaghan $E(V)$ equation of state [24] and obtain the variation shown in figure 1; the equilibrium lattice constant a_0 , bulk modulus B_0 and its pressure derivative B_0' are given in table 1. The values obtained with 70 Ryd and given in table 1 differ from the intermediate results calculated with 40 Ryd by $\leq 0.05 \text{ \AA}$, by $\approx 3 \text{ GPa}$

in zincblende and ≈ 30 GPa in rocksalt, and by ≈ 0.1 (dimensionless); we estimate that the errors due to the finite plane-wave cutoff are *smaller* or, at worst, equal to these differences. (The errors consequent to the pseudopotential method will be judged later, by comparing with the all-electron results.)

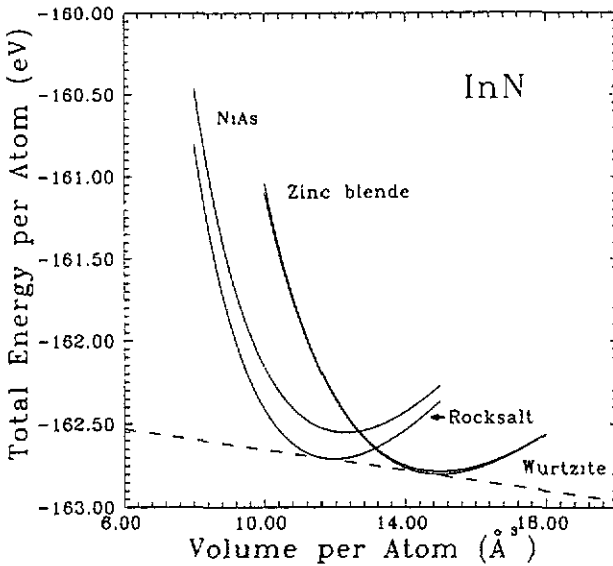


Figure 1. The $E(V)$ equations of state for the energetically most favourable modifications of InN. Full curves represent the density-functional pseudopotential calculations performed with a plane-wave cutoff $E^{PW} = 70$ Ryd and fitted with the Murnaghan equation of state; the FP-LMTO results are almost the same. The equations of state for the CsCl and A5 structures (not plotted) are, respectively, 0.96 and 1.50 eV per atom above the $E(V)$ of rocksalt. The common tangent (broken line) predicts the transition pressure from the wurtzite to rocksalt phase: 4.93 GPa at $T = 0$.

Table 1. Structural parameters and static properties of indium nitride, in different phases, as predicted by the pseudopotential PP and FP-LMTO calculations. High-pressure phase (rocksalt) and low-pressure phases (wurtzite, zincblende (metastable)). Lattice constants a_0 , c_0 and the internal distortion parameter u of the wurtzite structure, bulk modulus B_0 , its pressure derivative B'_0 , and the energy E_0 at static equilibrium. The FP-LMTO value of the bulk modulus in the wurtzite modification can be estimated at $B_0 \approx 143$ GPa.

	a_0 (Å)	c_0 (Å)	u	B_0 (GPa)	B'_0	E_0 (meV/atom)
wurtzite (PP)	3.483	5.7039	0.3767	166	3.8	-15.7
zincblende (PP)	4.931	—	—	161	4.1	0
zincblende (FP-LMTO)	4.929	—	—	138	3.9	0
rocksalt (PP)	4.574	—	—	213	4.4	+74.6
rocksalt (FP-LMTO)	4.578	—	—	191	3.9	+72.8
experiment (wurtzite)	3.5446 ^a	5.7034 ^a				
experiment (zincblende)	4.961 ^b	—				

^a [33].

^b [34].

In the next stage we deal with the wurtzite structure (four atoms per cell). Assuming that all In–N bonds have the same length as *calculated* in zincblende, one has the ‘ideal’ wurtzite structure with lattice constant $a = 3.487$ Å ($= a_{zbs}/\sqrt{2}$) and $c = 5.694$ Å (the ‘ideal’ ratio $c/a = \sqrt{8/3}$) and with no internal distortion ($u = 3/8$). It turns out that the energy of InN in this ‘ideal’ wurtzite structure is 12 meV per atom below that of ZBS. Starting from this configuration, and keeping the volume of the cell constant and $u = 0.375$, we first calculate

$E(a, c/a, u)$ for three different values of c/a and find the energy minimum. Then freezing a and c/a at 'best' values found, we vary the parameter u (four self-consistent calculations), and find the new minimum of $E(a, c/a, u)$. Finally, with c/a and u fixed at their 'optimized' values, we vary a and calculate $E(V) \equiv E(a, c/a, u)$ at seven different volumes V —which we fit, again, to the Murnaghan equation of state. The first two stages of this procedure were performed with a 40 Ryd cutoff, and only for the last step (the determination of $E(V)$) was the cutoff increased to 70 Ryd. The resulting structural parameters are summarized in table 1, together with other static properties obtained through Murnaghan fitting. The final $E(V)$ (figure 1) is only slightly (although discernibly) different from the one in which zincblende structure was assumed: the minimum E_0 in wurtzite is only 15.7 meV per atom lower than in ZBS, and one may conclude a possible coexistence of the two phases, with zincblende being the metastable state.

With InN in the rocksalt structure we proceed exactly as in the zincblende case, and obtain the data shown in figure 1 and table 1. In these calculations we assumed completely filled bands (semiconductor), and we checked that the structure was, indeed, *not* metallic: to this goal we employed the Gaussian smearing technique [25] for the k -space summation. We verified that the other possible structures, namely CsCl and A5 (the polar analogue of the β -Sn structure), lead to internal energies $E(V)$ situated far too high to be worth considering further (respectively 0.96 and 1.5 eV per atom above the rocksalt $E(V)$)†.

The fourth equation of state plotted in figure 1 corresponds to the NiAs-modification—an hexagonal structure with four atoms per cell, which can be thought of as an hexagonal analogue of rocksalt [26], as wurtzite is an hexagonal analogue of zincblende. Here we determined the $E(V)$ variation for four volumes V , and in each case the internal structural parameter was kept at the 'ideal' value. The k -space summation in the different phases (zincblende, wurtzite, rocksalt, NiAs, A5 and CsCl) was performed using, respectively, 10, 7, 10, 6, 12 and 4 'special points' which, in the Monkhorst–Pack [27] notation, correspond to $q_1q_2q_3 = 444$ for ZBS, NaCl and CsCl, to 442 for wurtzite and NiAs structures, and 224 for the A5.

From figure 1 one easily identifies the high-pressure structure of InN as the rocksalt modification—not surprisingly, considering the analogous result obtained for the other nitrides, GaN [11–13] and AlN [9, 10]. The slope of the common tangent to the two $E(V)$ curves (broken line) determines the wurtzite \rightarrow rocksalt transition pressure, which is given in table 2: $p_t = 4.93$ GPa. We estimate that the uncertainty of this value, consequent to the finite plane-wave cutoff, does not exceed 5%, i.e. ± 0.25 GPa at most ‡; also, we verified that the error resulting from the discrete sampling of the k -space is much smaller, namely of order 1.4%§. The main quantities characterizing the transitions are summarized in table 2: transition pressure, transition volumes V_t , and relative equilibrium energies of the phases; the *transition heat* can be obtained as $\Delta E = p_t \Delta V_t$. The fairly low transition pressure still has to be confirmed by experiment, but it compares well with the values, observed or calculated [28], in other indium compounds: 3.3 GPa in InSb and 8.4 GPa for InAs; less well with InP (12.8 GPa).

† As this conclusion was to be expected from analogy with all previous calculations on AlN and GaN [9–13], only the more modest cutoff of 40 Ryd was employed for this verification.

‡ For the analogous ZBS \rightarrow RS transition (which may be thought of as more accurately established, because any 'optimization' of the structural parameters is absent) we obtained 4.06 GPa at 70 Ryd and 4.26 GPa at 40 Ryd—meaning at most a 5% difference.

§ Rather than recalculate the entire $E(V)$ curves with the next larger set of 'special points', we checked the values of E_0 at the minima of the rocksalt and ZBS structures; the structural energy difference ΔE_0 obtained at 70 Ryd and with 28 'special points', was compared with the one calculated using 10 'special points' and given in table 1. It turned out that this improved sampling shifted the relative position of the rocksalt curve by merely -1.4% .

Table 2. Quantities referring to the wurtzite \rightarrow rocksalt and zincblende \rightarrow rocksalt phase transitions in indium nitride, as calculated by the pseudopotential (PP) and the FP-LMTO methods. Transition pressure p_t , transition volumes V_t and energy difference ΔE_0 between the minima of the two phases. The V_0 is the (calculated) equilibrium volume of the low-energy phase (wurtzite or zincblende; see data in table 1).

	p_t (GPa)	$V_t(\text{w or ZBS})/V_0$	$V_t(\text{RS})/V_0$	ΔE_0 (meV/atom)
wurtzite \rightarrow RS (PP)	4.93	0.972	0.781	+90.3
ZBS \rightarrow RS (PP)	4.06	0.976	0.784	+74.6
ZBS \rightarrow RS (FP-LMTO)	4.02	0.973	0.785	+72.8

4. Discussion

In order to verify the role of the $4d^{10}$ electrons in the In core, we repeated part of the procedures described above using the FP-LMTO method; we limited the comparison to *cubic* structures, where no optimization of the 'internal' structural parameters is necessary. In order to obtain physically meaningful equilibrium energies E_0 we have required the muffin-tin radii r_{In} and r_{N} to be equal in *both* structures when equilibria $E(V_0)$ are reached. Several repeated calculations of $E(V)$ were necessary, before arriving at the radii $r_{\text{In}} = r_{\text{N}} = 1.956 \text{ AU}$, fulfilling that condition, in both ZBS and RS structures, at the respective equilibrium volumes V_0 . These atomic spheres, together with the empty ones, fill 62.1% of the space in ZBS and 58.1% in rocksalt. The quantities derived from these calculations are quoted in tables 1 and 2 as well; the phase diagram, which looks very much like that in figure 1, is not plotted.

Perusal of the tables reveals that the effect of the d-electrons on the *structural* properties is about nil: both methods predict the same transition pressure (1% difference), and the calculated lattice constants agree to within 0.1% and better—suggesting that the uncertainties consequent to the finite number of plane-waves and given above are probably largely overestimated. The calculated structural parameters for wurtzite and ZBS are also in excellent agreement (1.5% to 0.1%) with those obtained in [29] by using different pseudopotential and with the nonlinear core correction [30] applied. On the contrary, the inclusion of the core electrons affects the *static* properties (essentially the bulk modulus B_0): the $\approx 10\%$ difference in rocksalt still could be an error caused by the plane waves, but the $\approx 15\%$ discrepancy in the predictions for B_0 in zincblende structure (and *a fortiori* in wurtzite structure) can only be explained by the neglect/inclusion of the $4d^{10}$ electrons. The best estimate for the wurtzite modification thus would be $B_0 = 143 \text{ GPa}$ —a value that can, in principle, be verified experimentally.

While waiting for experimental results it may be useful to examine the valence-charge distributions in the three (low- and high-pressure) modifications of InN (figure 2). In both structures the contour plots show nearly complete transfer of the valence charge from indium to nitrogen: the largest closed contour around In corresponds to only three electrons per cell, whereas the densities around N attain as much as ≈ 100 electrons per cell. In this respect the In–N bond (both in the RS and ZBS modifications), can be regarded as a prototype of the ideal ionic bonding. An interesting feature, worth noting, is that the maximum of the density is not situated at the nitrogen site itself, but $\approx 0.06a$ away from it; proceeding further to the centre, the density *decreases* and reaches only ≈ 10 electrons per cell at the site itself: the presence of the core showed here up, indirectly, through the *orthogonalization hole*.

Besides establishing that the rocksalt modification of InN is semiconducting, with a *direct* gap at the Γ point, we did not dwell on the details of the band structures: the well known gap problem of the local-density approximation would make most of the results

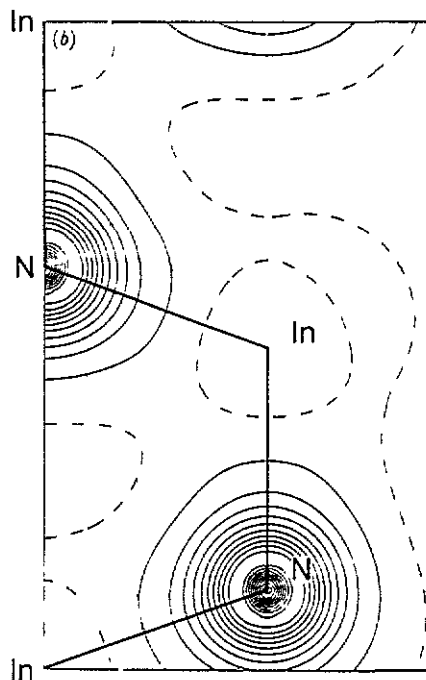
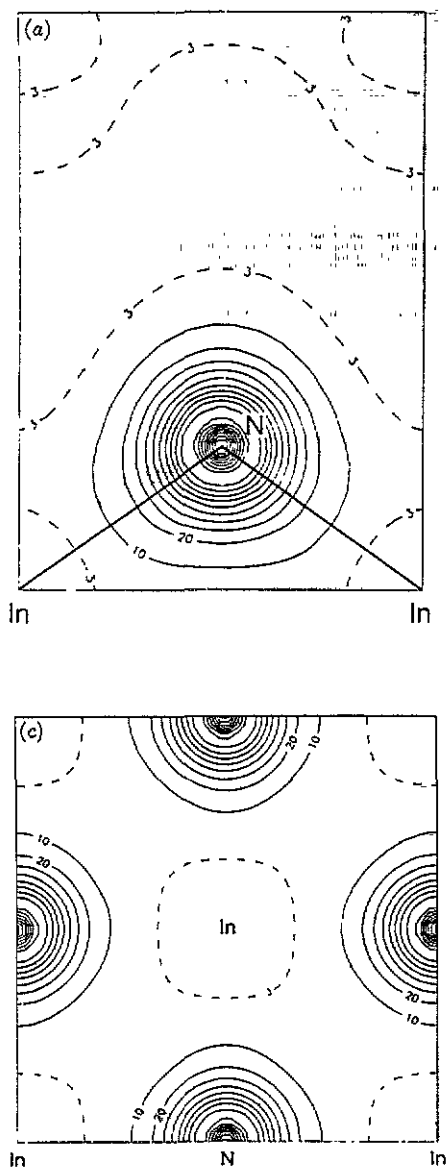


Figure 2. Distribution of the valence charge density calculated for InN in the low- and high-pressure modifications: (a) zincblende, (b) wurtzite and (c) rocksalt phase. The density is plotted (a), (b) in the plane (110), with the In–N bonds shown by full lines; (c) in the plane (100), with In atoms at the corners and in the centre of the square. Units: electrons per $(a^3/4)$, where $a = 4.574 \text{ \AA}$ for rocksalt and $a = 4.931 \text{ \AA}$ for zincblende and wurtzite (equivalent volume). The contour step is ten, and an extra contour 3 (broken curve) is displayed around the In site, which is deprived of almost all electrons. In all modifications nearly all valence charge accumulates around the nitrogen. The density increases until 108 is reached in zbs/wurtzite and 86 in rocksalt (no particular mark on the figure); the highest displayed contour 100 (or 80) is thus followed by one more contour 100 (or 80), the density then *decreases* sharply, and reaches 10 at the very centre of nitrogen ('orthogonalization hole').

worthless. The band structure of the wurtzite modification of InN has already been studied, using the empirical pseudopotential method, by Foley and Tansley [31].

Returning to the question of trends one may wonder whether a knowledge of p_t for InN affords any clues. We see that the InN placed itself, on the scale of transition pressures, exactly where common sense would suggest it belongs, namely at the lowest end of the series BN—AlN—GaN—InN. The anticipated monotonic decrease in p_t is disobeyed by the pair AlN, GaN for which the tendency is reversed; one could also view this as a trend *broken* at Al/Ga. Inspection of other III–V compounds reveals, however, that the same 'Al \leftrightarrow Ga reversal' is also found in phosphides, arsenides and antimonides (figure 3), which in itself constitutes a definite trend: the particularity of nitrides consists in an exaggeration of the tendency observed in *all* III–V compounds.

The reasons for the above 'reversal' can only be speculated about. The most obvious difference between Al and Ga consists, of course, in taking in the d-electrons into the core. Before suspecting any polarization of the core, the simplest explanation of the Al, Ga difference consists in noticing one direct consequence of merely the *presence* of the d-electrons, namely the size of the valence s and p orbitals, as measured, for example, by the position of the outermost peak of the radial wavefunctions [29]: this size increases with the atomic number, from B to In by a factor 1.4 (s orbital) to 1.8 (p orbital). The sizes of both Al and Ga are situated in between, but the orbitals *shrink* when going from Al to Ga (namely, by 9% (s orbital) and 5% (p orbital))! The break in monotonicity at the Al/Ga point thus already exists at the level of atomic orbitals. Similar behaviour as in figure 3 was recently observed [32], with all four III-V series, in the behaviour of the equilibrium energy difference $E_0(\text{wurtzite}) - E_0(\text{ZBS})$, and it is likely that it would be reproduced if the $E_0(\text{RS}) - E_0(\text{ZBS})$ were plotted in figure 3 instead of p_t .

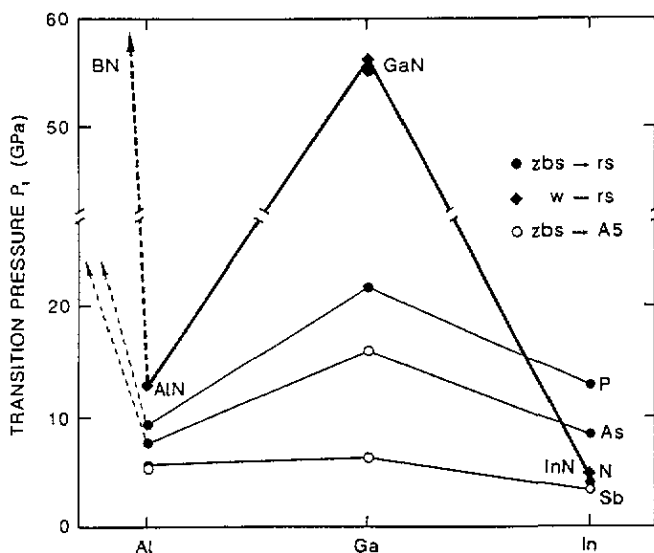


Figure 3. Transition pressure of the nitrides, in the context of other III-V compounds, as obtained from the density-functional pseudopotential calculations of [9, 11, 26, 28] and in this work.

5. Conclusions

In summary, we have identified the high-pressure phase of indium nitride to appear as rocksalt structure, and to be semiconducting; the transition pressure wurtzite \rightarrow rocksalt is predicted to be 4.93 GPa at $T = 0$. We also supplied a few missing pieces of information on structural and static properties of the low-pressure phase (wurtzite): the internal distortion parameter u , the bulk modulus B_0 and its pressure derivative B'_0 . The influence of the core-electrons on the structural properties (a_0 and p_t) is about nil, but the $4d^{10}$ electrons of In may be responsible for the $\approx 15\%$ difference in the bulk moduli B_0 predicted by the pseudopotential and the FP-LMTO methods.

Acknowledgments

We wish to thank M Methfessel for offering us access to the codes materializing the full-potential LMTO method. We are grateful to M Besson and A Polian for informing us about their experimental work prior to publication, and to S Froyen for useful discussion. This study was accomplished within the Franco-Spanish collaboration program 'Acción Integrada'. One of us (AM) wishes to thank the Gobierno Autónomo Canario for partial financial support. The computer resources were provided by the Scientific Committee of the CCVR (Centre de Calcul Vectoriel pour la Recherche), Palaiseau, France.

References

- [1] Knittle E, Wentzcovitch R M, Jeanloz R and Cohen M L 1989 *Nature* **337** 349
- [2] Vollstädt H, Ito E, Akaishi M, Akimoto S, Fukunaga M J A and Fukunaga O 1990 *Proc. Japan. Acad. B* **66** 7
- [3] Ueno M, Onodera A, Shimomura O and Takemura K 1992 *Phys. Rev. B* **45** 10123
- [4] Perlín P, Jaubertie-Carillon C, Itie J P, San Miguel A, Grzegory I and Polian A 1991 *High Pressure Res.* **7** 96; 1992 *Phys. Rev. B* **45** 83
- [5] Ching W Y and Harmon B N 1986 *Phys. Rev. B* **34** 5305
- [6] Wentzcovitch R M, Chang K J and Cohen M L 1986 *Phys. Rev. B* **34** 1071
- [7] Wentzcovitch R M, Cohen M L and Lam P K 1987 *Phys. Rev. B* **36** 6058
- [8] Nielsen O H and Kunc K 1991 *Festschrift in honor of R C Leite* ed M Balkanski, C E T Gonçalves da Silva and J M Worlock (Singapore: World Scientific) pp 112–23
- [9] Van Camp P E, Van Doren V E and Devreese J T 1991 *Phys. Rev. B* **44** 9056
- [10] Gorczyca I, Christensen N E, Perlín P, Grzegory I, Jun J and Bockowski M 1991 *Solid State Commun.* **79** 1033
- [11] Muñoz A and Kunc K 1991 *Phys. Rev. B* **44** 10372
- [12] Gorczyca I and Christensen N E 1991 *Solid State Commun.* **80** 335
- [13] Van Camp P E, Van Doren V E and Devreese J T 1992 *Solid State Commun.* **81** 23
- [14] Chelikowsky J R 1987 *Phys. Rev. B* **35** 1174
- [15] Polian A and M Besson 1992 private communication
- [16] Kohn W and Sham L J 1965 *Phys. Rev.* **140** A1133
Sham L J and Kohn W 1966 *Phys. Rev.* **145** B561
- [17] Bachelet G B, Hamann D R and Schlüter M 1982 *Phys. Rev. B* **26** 4199
- [18] Ceperley D M and Alder B J 1980 *Phys. Rev. Lett.* **45** 566
Perdew J and Zunger A 1981 *Phys. Rev. B* **23** 5048
- [19] Min B J, Chan C T and Ho K M 1992 *Phys. Rev. B* **45** 1159
- [20] Methfessel M 1988 *Phys. Rev. B* **38** 1537
- [21] Andersen O K, Jepsen O and Glötzel D 1985 *Highlights of Condensed Matter Theory* ed F Bassani, F Fumi and M Tosi (Amsterdam: North Holland)
- [22] Fiorentini V, Methfessel M and Scheffler M 1993 *Phys. Rev. B* **47** 13353
- [23] Hedin L and Lundqvist B I 1971 *J. Phys. C: Solid State Phys.* **4** 2064
- [24] Mumaghan F D 1944 *Proc. Nat. Acad. Sci. USA* **50** 697
- [25] Fu C L and Ho K M 1983 *Phys. Rev. B* **28** 5480
Needs R J, Martin R M and Nielsen O H 1986 *Phys. Rev. B* **33** 3778
- [26] Froyen S and Cohen M L 1983 *Phys. Rev. B* **28** 3258
- [27] Monkhorst H J and Pack J D 1976 *Phys. Rev. B* **13** 5188
- [28] Zhang S B and Cohen M L 1987 *Phys. Rev. B* **35** 7604
- [29] Chin-Yu Yeh, Lu Z W, Froyen S and Zunger A 1992 *Phys. Rev. B* **46** 10086
- [30] Louie S G, Froyen S and Cohen M L 1982 *Phys. Rev. B* **26** 1738
- [31] Foley C P and Tansley T L 1986 *Phys. Rev. B* **33** 1430
- [32] Chin-Yu Yeh, Lu Z W, Froyen S and Zunger A 1992 *Phys. Rev. B* **45** 12130
- [33] Pichugin I G and Tlachala M 1978 *Izv. Akad. Nauk SSSR, Neorg. Mater.* **14** 175
- [34] Strite S, Ruan J, Smith D J, Sanel J, Manning N, Chen H, Choyke W J and Morkoç H 1992 *Bull. Am. Phys. Soc.* **37** 346